NUCLEIC ACID THERAPEUTICS
Volume 30, Number 4, 2020
Mary Ann Liebert, Inc.
DOI: 10.1089/nat.2020.0847

# Likelihood of Nonspecific Activity of Gapmer Antisense Oligonucleotides Is Associated with Relative Hybridization Free Energy

Andrew T. Watt, Grant Swayze, Eric E. Swayze, and Susan M. Freier

Reduction of matched and nearly complementary unintended transcripts was evaluated for 96 antisense oligonucleotides (ASOs) and 832 nearly matched unintended transcripts. The ASOs were 16–20 nucleotide ''gapmers'' with a gap of 8–10 DNA residues and 2′-O-methoxy-ethyl or constrained-ethyl substitutions in the wings. Most unintended transcripts were not reduced or were reduced with a potency more than 10-fold weaker than the intended transcript. For the unintended transcripts that were reduced, a strong correlation between relative potency of the intended versus the unintended transcript with predicted free energy of hybridization was observed. These results suggest ASO selectivity should be evaluated by testing for reduction of the unintended transcripts predicted to bind most stably to the ASO.

**Keywords:** antisense oligonucleotides, hybridization thermodynamics, unintended targets

## Introduction

Nucleic acid therapeutics exploit the exquisite specificity of Watson–Crick hybridization and have recently resulted in approval of drugs for previously untreatable diseases [1–4]. Whether the goal is therapeutic benefit, or determining the function of a novel gene, affecting the transcript without direct effect on other gene products is preferred and a method for identifying selective compounds with no effect on unintended transcripts is desired.

Despite the high selectivity of Watson–Crick hybridization, antisense oligonucleotides (ASOs), small interfering RNAs (siRNAs), CRISPR guide RNAs (sgRNAs), and ribozymes can bind to nearly complementary unintended transcript sites with the potential of activity at those sites. Specificity of these compounds as well as specificity of nucleic acid probes has been the subject of much research [5–26].

Although early studies with mismatched ASOs showed antisense activity decreased with increasing mismatches [27], antisense activity at nearly matched sites has been reported [7,8]. These nearly complementary sites in the transcriptome can be identified *in silico* using sequence alignment tools [28–32]. For any ASO, not all these nearly matched sites are effectively reduced, so methods for predicting activity of an ASO at a nearly matched nonintended site would be useful to allow for design of ASOs with minimal off-target activity.

The most widely used mechanism for ASO inhibition of gene expression requires hybridization of the ASO to its complementary RNA target followed by RNase H1 cleavage of the RNA. Selectivity against an unintended transcript will be observed if either hybridization or RNase H1 cleavage is less efficient at the unintended nearly complementary site compared with the intended target site. The study described below evaluates activity of ASOs against nearly complementary unintended transcripts and the role of hybridization thermodynamics in specificity of ASOs.

Prior studies evaluating reduction of unintended transcripts by ASOs suggest near complementary of an ASO, with its unintended transcript associated with reduction of that unintended transcript. Kamola *et al.* evaluated six locked nucleic acid (LNA) gapmer ASOs for reduction of a handful of mismatched unintended targets [8]. They reported a correlation between $T_M$ of the ASO:target duplex and degree of reduction at a single concentration.

Rukov *et al.* tested two LNA gapmers for selective reduction of a library containing randomized 7-mer target sites [6], and demonstrated a correlation of binding score with activity at mismatched sites. Hagedorn *et al.* tested four LNA gapmers for reduction of unintended transcripts in mouse liver [7]. They

Division of Antisense Research, Ionis Pharmaceuticals, Carlsbad, California, USA.

demonstrated fewer mismatches in the ASO:target duplex resulted in a higher chance of reduction of that transcript.

Yoshida *et al.* [9] used microarrays to test two short LNA gapmers for reduction of unintended targets in human cells and found a strong correlation of number of mismatches with likelihood of off-target reduction. These prior experiments used relatively few numbers of ASOs. Furthermore, they evaluated selectivity by comparing transcript reduction at a single, relatively high concentration of ASO so relative potency comparing intended to unintended transcript could not be measured.

We report below the evaluation of 96 ASOs for reduction of unintended transcripts and the correlation of the reduction of 832 unintended transcripts with mismatch destabilization energies. The number of ASO:transcript pairs tested and these detailed comparisons of potency differences for intended versus unintended transcripts allowed us to demonstrate high correlation between binding of the ASO to the mismatched target site and the likelihood of activity at that unintended target site.

## Materials and Methods

### *Oligonucleotides*

ASOs were synthesized using standard phosphoramidite chemistry as described previously [33]. RNA oligonucleotides were purchased from Integrated DNA Technologies, Coralville, Iowa.

### In silico *analysis of predicted off-target matches in the human transcriptome*

The sequence of each ASO was aligned against the reference human transcriptome (hg38/GRCh38|Assembly) containing all gene sequence and all processed transcripts defined by NCBI's Reference Sequence Database listing (www.ncbi.nlm.nih.gov/refseq/) (Release 76, May 9, 2016). Alignment was performed using Bowtie [29]. Alignments for ASOs of length 20 were filtered to allow for up to 2 mismatches anywhere or up to 3 terminal mismatches with 17 matches in a row. For 16-mers, the bowtie filter was a maximum of 1 mismatch anywhere or 2 terminal mismatches with 14 matches in a row.

### *Cell culture and ASO treatment*

Many of the unintended transcripts were not expressed in routinely used cell lines so eight cell lines were required for this study. Most cells were purchased from ATCC (Manassas, VA) and cultured at 37°C as described in Supplementary Table S1. Culture conditions, transfection methods, and treatment times are described in Supplementary Table S1.

For free uptake transfection, the cells were counted and diluted in room temperature growth medium to the indicated concentration before adding 100 μL of the cell suspension to the wells of a collagen I-coated 96-well culture plate (354407, Corning, Inc., Corning, NY). Immediately after plating the cells, 11 μL of 10× oligonucleotide in water was added to the appropriate wells and the culture plate was incubated at the indicated conditions. After 48 h, the cells were washed once with phosphate-buffered saline (PBS) before lysing for RNA isolation and analysis.

For cells requiring electroporation, cells were trypsinized, counted, and diluted in room temperature growth medium before adding 100 μL of the cell suspension to the wells of a 2 mm electroporation plate (45-0450-M; BTX, Holliston, MA), which contained 11 μL of 10× oligonucleotide in water. After shaking the plate for 30 s, the cells were pulsed once at the indicated voltage for 6 ms with the ECM 830 instrument (BTX). After electroporation, the cells were transferred to a Corning Primeria 96-well culture plate (353872; Corning, Inc.) containing 50 μL of growth medium and incubated at the indicated conditions. After 24 h, the cells were washed 1× with PBS before lysing for RNA isolation and analysis.

iCell™ neurons purchased from Cellular Dynamics were plated and cultured in 96-well poly-ornithine/laminin-coated plates following the manufacturer's instructions using iCell neuron maintenance medium (NRM-100-121-001) and iCell neuron medium supplement (NRM-100-031-001). Twenty-four hours after plating, the cells were refed with 50 μL of complete maintenance medium containing 2× oligonucleotide and returned to the incubator. On the second and fourth day after plating, 100 μL of complete maintenance medium was added to each well. Six days after plating, the cells were washed 1× with PBS and lysed for RNA purification and analysis.

For most of the unintended transcripts, both the intended and unintended transcript levels were measured on a single RNA sample from each biological replicate. In a few cases, the intended transcript and unintended transcript were not expressed in the same cell line. In that case, a surrogate ASO targeting human *ACTN1* (ASO_099) was tested in both cell lines and its potency was used to predict potency of both the intended and unintended transcript in the cell line in which they were not expressed.

### *RNA purification and analysis*

RNA was purified with a glass fiber filter plate (Pall 5072) and chaotropic salts with on-column DNAseI digestion. Levels of mRNA were quantitated with quantitative reverse transcription polymerase chain reaction (RT-qPCR) on the QS7 instrument (Applied Biosystems). Briefly, 5–10 μL RT-qPCRs containing 0.4–4 μL of RNA were run with AgPath-ID™ One-Step RT-PCR Reagents (AM1005; Life Technologies, Carlsbad, CA) and the primer-probe sets listed in Supplementary Table S2 following the manufacturer's instructions. Total RNA levels were measured with Quant-iT™ RiboGreen® RNA reagent (R11491; Life Technologies). Total RNA was used to normalize the transcript expression results. For some samples, GAPHDH expression levels were measured by RT-qPCR and also used to normalize expression. In all cases, normalization by total RNA agreed with normalization by GAPDH.

### *$IC_{50}$ determination*

For most of the ASOs studied, cells were treated in quadruplicate at five or six concentrations in a series of four or five-fold serial dilutions. A few of the unintended transcript pairs were measured only in duplicate. The highest concentration was at least 10 times the $IC_{50}$ of the intended transcript. Concentration response data normalized to untreated control were analyzed using nonlinear regression (GraphPad Prism).

### *$\Delta G^\circ_{37}$ predictions*

$\Delta G^\circ_{37}$ for RNA:RNA duplexes were predicted using RNAstructure [34].

### *$T_M$ measurements*

ASO was combined with RNA oligonucleotide corresponding to each predicted off-target at 4 μM each strand. All RNA oligonucleotides contained a ''dangling end'' on each end of the complementary region corresponding to the sequence of the predicted off-target gene at that site. $T_M$ of the ASO:RNA duplex was measured at 260 nm in 100 mM $Na^+$, 10 mM phosphate, 0.1 mM EDTA, pH 7.0. $T_M$ was also measured for the RNA analog of each ASO binding to the same RNA target.

## Results and Discussion

### *Mismatch destabilization of an ASO:RNA duplex correlated strongly with the predicted RNA:RNA destabilization*

To test the hypothesis that unintended targets with stronger hybridization potential are more likely to be reduced than those with destabilizing mismatches, hybridization free energies for matched and mismatched ASOs binding to RNA targets are required. Although algorithms are available for predicting stability of PNA:DNA and LNA:DNA hybrids and the effect of LNA substitution on the stability of 2′-O-Methyl:RNA duplexes [35–41], hybridization free energies cannot be accurately predicted for complexes between modified gapmer ASOs and RNA.

To assess thermodynamic stability of ASO:RNA duplexes, $T_M$ was measured for 25 ASOs to a total of 153 matched and mismatched target sequences. Similar measurements were performed for RNA analogs of each of the 25 ASOs to the same RNA targets. Sequences of these oligonucleotides and the $T_M$s are listed in Supplementary Table S3. $T_M$s of the ASO:RNA duplex correlated well with those of RNA:RNA duplex and, in fact, the correlation was similar whether the ASO was a 20-mer with 2′-O-methoxy-ethyl (MOE) in the wings or a 16-mer with 2′-O-cEt in the wings (Supplementary Fig. S1).

$T_M$ accurately measures $\Delta G^{\circ}$ at the $T_M$ but extrapolation from the $T_M$ to 37°C requires knowledge of the enthalpy of duplex formation. According to the two-state model, the free energy of duplex formation at 37°C is given by:

$$\Delta G^{\circ}_{37} = \Delta H^{\circ}(1 - 310.15/T_M) + 310.15 \times R \times \ln(C_T/4)$$

where $\Delta H^{\circ}$ is the enthalpy of duplex formation, $T_M$ is the duplex melting temperature in °K, $R$ is the universal gas constant (1.987 cal/mol/deg) and $C_T$ is the total strand concentration at which $T_M$ was measured.

For each duplex structure, matched or mismatched, $\Delta H^{\circ}$ was calculated using the nearest-neighbor parameters of Turner and Mathews [42] and used to convert $T_M$ to $\Delta G^{\circ}_{37}$. Free energy of duplex destabilization ($\Delta\Delta G^{\circ}_{37}$) was calculated by subtraction of the free energy of the match from that of the mismatch.

Figure 1 plots the free energy destabilization for each mismatched ASO:RNA duplex versus that of the RNA:RNA duplex. A very high correlation was observed. The absolute stability of an ASO:RNA duplex differed from that of the RNA:RNA ortholog due to chemical modifications but the destabilization free energy due to the mismatch was very similar for RNA:RNA duplexes and ASO:RNA duplexes.

There is some question if $\Delta H^{\circ}$ from the nearest-neighbor model for RNA:RNA duplexes in 1 M NaCl is appropriate for

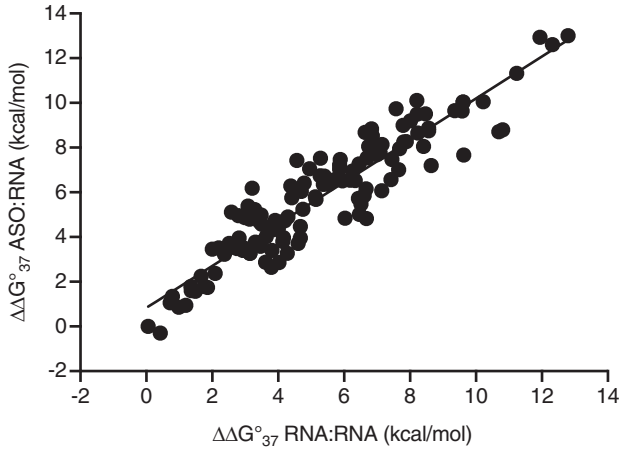


**FIG. 1.** Free energy destabilization of an ASO binding to an unintended target versus that of the equivalent RNA binding to the same RNA target. $\Delta\Delta G^{\circ}_{37}$ was calculated from the observed $T_M$ and $\Delta H^{\circ}$ calculated for the matched or mismatched RNA using nearest neighbor parameters of Turner and Mathews. ASO, antisense oligonucleotide.

extrapolating from $\Delta G^{\circ}$ at the Tm to $\Delta G^{\circ}_{37}$ for RNA:RNA duplexes and ASO:RNA duplexes in 100 mM NaCl. $\Delta H^{\circ}$ determined at 1 M NaCl can be used to extrapolate $\Delta G^{\circ}$ in 100 mM NaCl because the effect of ionic strength on duplex stability is primarily entropic, so $\Delta H^{\circ}$ is independent of salt concentration [43,44]. To test if the $\Delta H^{\circ}$ for RNA:RNA is also appropriate for ASO:RNA duplexes, $\Delta H^{\circ}$ was also obtained from the shape of the experimental melting curves using a standard six parameter fit [45]. When $\Delta G^{\circ}_{TM}$ and the fitted $\Delta H^{\circ}$ were used to compute $\Delta\Delta G^{\circ}_{37}$, data agreed with those in Fig. 1 in support of the assumption that nearest-neighbor values for $\Delta H^{\circ}$ are appropriate for both ASO:RNA and RNA:RNA duplexes (Supplementary Fig. S2).

Figure 2 compares the observed $\Delta\Delta G^{\circ}_{37}$ for these mismatched pairs to the $\Delta\Delta G^{\circ}_{37}$ for an RNA:RNA duplex predicted by RNAstructure [34]. The $\Delta G^{\circ}_{37}$ for duplex formation

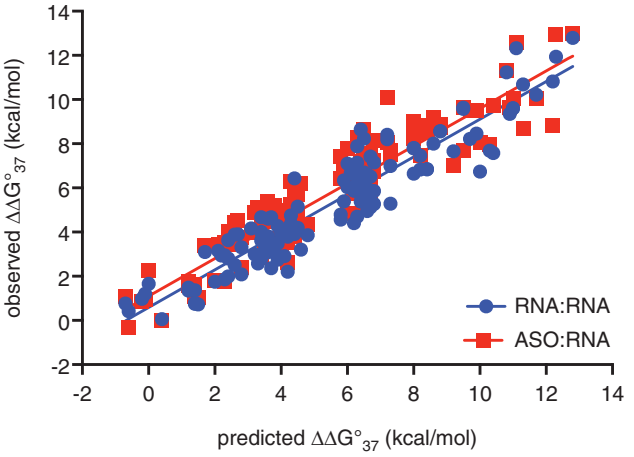


**FIG. 2.** The observed destabilization for ASOs binding to an unintended RNA target versus that predicted for the corresponding RNA:RNA duplex (*red*). Observed destabilization for the equivalent RNA:RNA duplexes is shown in *blue*.

calculated using RNAstructure was typically much more favorable than that observed in our $T_M$ experiments, probably due to the reduced ionic strength in the $T_M$ experiments and ASO duplex destabilization due to phosphorothioate linkages. However, the destabilization free energy ($\Delta\Delta G°_{37}$) observed in the $T_M$ experiments correlated strongly with the mismatch destabilization free energy predicted by RNAstructure. These data support the hypothesis that mismatch destabilization predicted by RNAstructure is an accurate estimate of the mismatch destabilization of an ASO:RNA duplex regardless of ASO length or chemical modification.

This correlation of the observed $\Delta\Delta G°_{37}$ for an ASO:RNA hybrid with the $\Delta\Delta G°_{37}$ predicted by RNAstructure for an RNA:RNA duplex allowed us to use the algorithms for prediction of RNA:RNA duplex stability developed from nearly 50 years of thermodynamic studies [42,46,47] to predict destabilization free energies for chemically modified ASOs. Lindow and colleagues [6,7] also used thermodynamic parameters for RNA:RNA duplexes to predict free energy differences for LNA gapmers binding to matched and mismatched targets. Although they did not directly measure duplex free energies for the LNA gapmers, our results support their assumption that RNA:RNA thermodynamic parameters are good predictors of mismatch destabilization in ASO:RNA duplexes.

Nearest-neighbor parameters can even be used to predict duplex stability under conditions similar to those inside a cell. Ghosh *et al.* recently reported that relative stabilities of nucleic acid duplexes under conditions of molecular crowding were similar to those in dilute buffer [48] suggesting that our rules for predicting mismatch destabilization of ASO:target pairs may even extend to the intracellular environment.

### *Most predicted mismatch pairs showed at least 10-fold selectivity for the intended transcript*

Ninety-six ASOs to 10 different transcribed genes were selected for evaluation of effects on unintended transcripts. The ASOs ranged in length from 16 to 20 nucleotides with a majority of 16-mers. All ASOs were DNA-gapmers containing a gap of 8–10 DNA residues flanked by wings of 2′-O-modified residues, 2′-O-MOE for the 20-mers, and constrained ethyl (cEt) for the 16-mers [49,50]. These 96 ASOs were selected because they were very active against their intended transcripts *in vitro* and *in vivo* and showed no hepatotoxicity or immune stimulation in standard rodent toxicology studies. ASOs tested are listed in Supplementary Table S4.

For each ASO, the human transcriptome was computationally searched for mismatched RNA target sites. Both primary and processed transcripts were interrogated. Concentration dependence of reduction of intended transcript and several matched or nearly matched unintended transcripts was measured in ASO-treated cells, so all transcripts were full-length human transcripts in their natural cellular context. RT-qPCR was selected to measure reduction of intended and unintended transcripts due to its very high sensitivity and accuracy.

Measurement of the concentration dependence of transcript reduction for every intended or unintended transcript at ASO concentrations up to 10 times the $IC_{50}$ of the intended transcript allowed for identification of unintended target transcripts with $IC_{50}$ up to 10-fold less potent than the intended transcript. Such detailed dose/response is required to predict the relative activity against intended and unintended transcripts at concentrations likely to occur *in vivo*. This exercise resulted in dose/response curves for 832 pairs of an ASO with an unintended transcript. $IC_{50}$ values for both the intended and unintended transcripts were determined from the dose/response and the ratio of $IC_{50}$ (unintended) to $IC_{50}$ (intended) was determined. Data are tabulated in Supplementary Table S5. ASO_112 and ASO_113 were used as negative controls and neither reduced any target below 80% control at any concentration up to 10×the $IC_{50}$ of the intended target.

Figure 3 shows examples of dose/response curves for mismatched transcripts of ASO_001 measured in A431 cells using TaqMan RT-qPCR. Unintended targets were identified as sites in the human transcriptome with up to one internal or two terminal mismatches to the ASO. Table 1 lists mismatch structures and $IC_{50}$ values for the intended and each unintended target site. ASO_001 is a rather promiscuous 16-mer ASO; the $IC_{50}$ for *REV3L* was only 2-fold weaker than that for the intended transcript, and those for *CACNA2D1* and *CLASP1* were slightly more than 10-fold less potent than *EZH2*, the intended target transcript. All three of the unintended transcripts that were reduced contained only terminal mismatches to the ASO. Other unintended transcripts with internal or terminal mismatches were even less potent.

Similar data for ASO_053 are shown in Supplementary Fig. S4 with mismatched structures and $IC_{50}$ ratios in Supplementary Table S6. For this 16-mer, none of the 28 unintended transcripts was reduced with $IC_{50}$ within 10-fold that of the intended transcript. Data for ASO_029, a 20-mer, are shown in Supplementary Fig. S5 and Supplementary Table S7. For this 20-mer, unintended target sites were identified as sites in the human transcriptome with up to two internal or three terminal mismatches to the ASO and none of the unintended transcripts was reduced.

Figure 4a plots the distribution of activity among these 832 unintended target transcripts. Only 97 of the pairs (12%) showed potency within 10-fold that of the intended transcript;

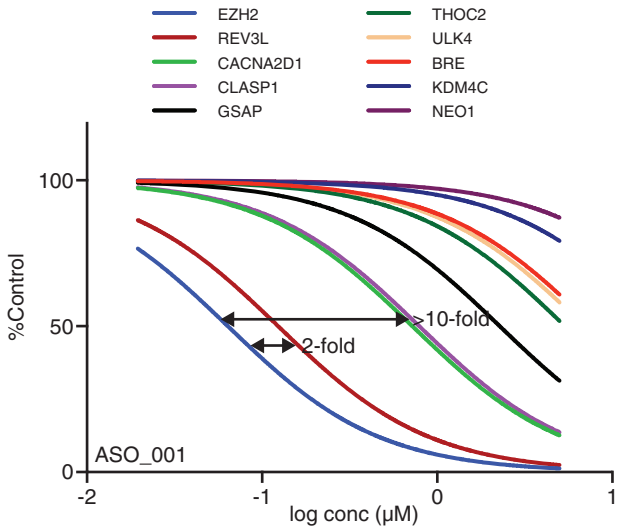


**FIG. 3.** Dose/response curves for nine unintended target transcripts of ASO_001, a 3-10-3 gapmer with 2′-cEt wings. Only fitted curves are graphed. Supplementary Figure S3 shows the same data with data points and error bars. $IC_{50}$ ratios and destabilization free energies for these pairs are shown in Table 1.

Table 1. Mismatch Structure, $IC_{50}$, and Predicted Destabilization Free Energy of the Unintended Target Sites of ASO_001 in Figure 3

| *ASO:target* | *Target sequence*[a] | *$IC_{50}$ (μM)* | *$IC_{50}$ ratio*[b] | *$\Delta\Delta G°_{37}$*[c] *(kcal/mol)* |
|---|---|---|---|---|
| ASO_001 | 5′ ATCATTATATTGACCA 3′ | | | 0.0 |
| | \|\|\|\|\|\|\|\|\|\|\|\|\|\|\|\| | | | |
| *EZH2* | 3′GUAGUAAUAUAACUGGUU 5′ | 0.064 | | |
| ASO_001 | 5′ ATCATTATATTGACCA 3′ | | | 0.9 |
| | \|\|\|\|\|\|\|\|\|\|\|\|\|\|\|**x** | | | |
| *REV3L* | 3′UUAGUAAUAUAACUGGCU 5′ | 0.124 | 1.94 | |
| ASO_001 | 5′ ATCATTATATTGACCA 3′ | | | 0.3 |
| | \|\|\|\|\|\|\|\|\|\|\|\|\|\|\|**x** | | | |
| *CACNA2D1* | 3′AUAGUAAUAUAACUGGAA 5′ | 0.722 | 11.3 | |
| ASO_001 | 5′ ATCATTATATTGACCA 3′ | | | 1.3 |
| | **x**\|\|\|\|\|\|\|\|\|\|\|\|\|\|\|**x** | | | |
| *CLASP1* | 3′AAAGUAAUAUAACUGGAU 5′ | 0.791 | 12.4 | |
| ASO_001 | 5′ ATCATTATATTGACCA 3′ | | | 2.9 |
| | **xx** \|\|\|\|\|\|\|\|\|\|\|\|\|\| | | | |
| *GSAP* | 3′UAUGUAAUAUAACUGGUA 5′ | 2.28 | 35.7 | |
| ASO_001 | 5′ ATCATTATATTGACCA 3′ | | | 4.3 |
| | \|\|\|\|\|\|\|\|\|\|\|\|\|**x**\| | | | |
| *THOC2* | 3′GUAGUAAUAUAACUGUUT 5′ | >5 | >50 | |
| ASO_001 | 5′ ATCATTATATTGACCA 3′ | | | 2.8 |
| | \|\|\|\|\|\|\|\|\|\|X\|\|\|\| | | | |
| *ULK4* | 3′CUAGUAAUAUAAUUGGUG 5′ | >5 | >50 | |
| ASO_001 | 5′ ATCATTATATTGACCA 3′ | | | 2.2 |
| | **xx**\|\|\|\|\|\|\|\|\|\|\|\|\|\|\| | | | |
| *BRE* | 3′AAGGUAAUAUAACUGGUG 5′ | >5 | >50 | |
| ASO_001 | 5′ ATCATTATATTGACCA 3′ | | | 4.7 |
| | \|\|\|\|\|\|\|\|\|\|\|\|\|\|\|**x**\| | | | |
| *KDM4C* | 3′UUAGUAAUAUAACUGAUG 5′ | >5 | >50 | |
| ASO_001 | 5′ ATCATTATATTGACCA 3′ | | | 4.3 |
| | \|\|\|\|\|\|**x**\|\|\|\|\|\|\|\|\|\| | | | |
| *NEO1* | 3′GUAGUAAGAUAACUGGUU 5′ | >5 | >50 | |

[a]Mismatched binding site on target RNA, including one additional nucleotide on each end. Upper strand is ASO and lower strand is RNA target site. Sites of mismatch are in *bold*.
[b]$IC_{50}$ (unintended transcript)/$IC_{50}$ (intended transcript).
[c]$\Delta G°_{37}$ (unintended target site) − $\Delta G°_{37}$ (intended target site).
ASO, antisense oligonucleotide.

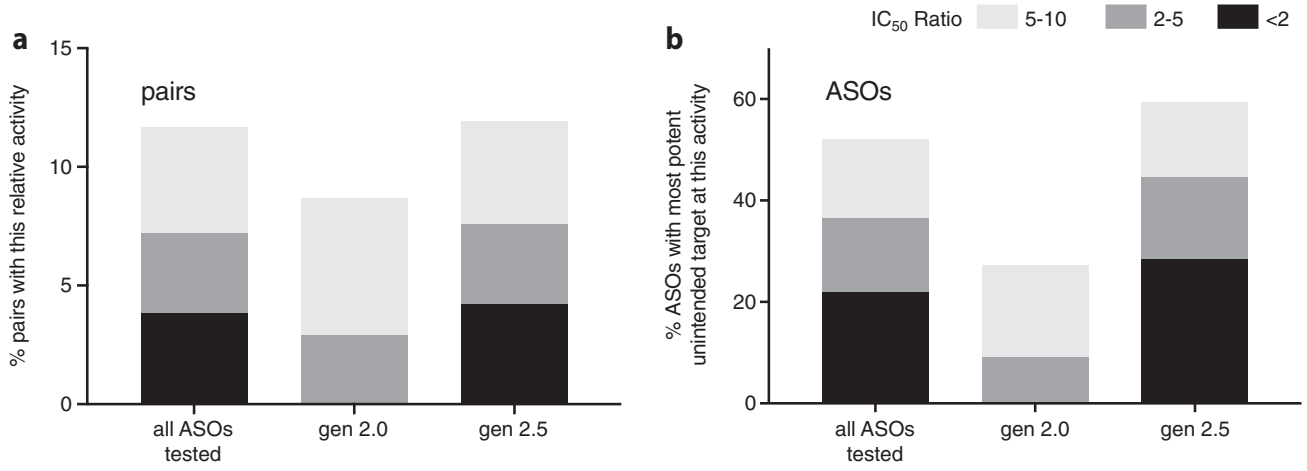


**FIG. 4.** Distribution of activity of 96 ASOs tested against 832 unintended transcripts. Indicated ratio is the $IC_{50}$ for the unintended transcript relative to that of the intended transcript. Unintended transcripts with ratio <2 are nearly as potent as the intended transcript; ratio ≥10 indicates little or no measurable reduction of the unintended transcript. **(a)** Fraction of ASO-unintended target pairs with potency within 2-, 5- or 10-fold that of the intended target. **(b)** Fraction of ASOs tested with the most potent unintended target within 2-, 5-, or 10-fold that of the intended target. In both panels, the first column represents all 96 ASOs tested and the other columns separate the ASOs into gen 2.0 (mostly 20 nt MOE gapmers) and gen 2.5 (16 nt cEt gapmers). MOE, methoxyethyl.

60 (7.2%) of these were within 5-fold, and 32 (3.8%) were within 2-fold of the intended transcript.

Figure 4b plots the likelihood an ASO will have any potent unintended target; 48% of the ASOs tested had no unintended targets reduced with a potency within 10×that of the intended target. When the analysis was restricted to 20 nt MOE gapmers, fully 73% of the ASOs tested had no unintended targets reduced with potency within 10×that of the intended target. $T_M$s of the matched 20-mer MOE compounds were similar to those of the matched 16-mers containing cEt substitutions (Supplementary Table S3) suggesting that the affinity of these two classes of compounds for their intended targets is similar. Yet the 20-mers reduced many fewer unintended targets than the 16-mer ASOs. This is likely due to the fact that the number of single (or double) mismatched sites in the human transcriptome is substantially higher for a 16-mer than a 20-mer, so the probability of finding an unintended site with a small $\Delta\Delta G°_{37}$ is much lower for a 20-mer than a 16-mer.

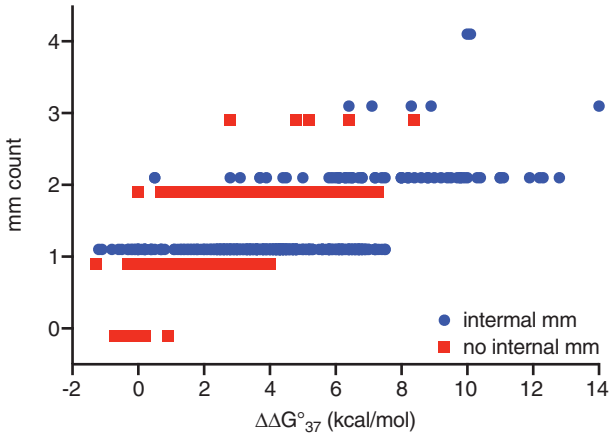


**FIG. 5.** Distribution of destabilization free energy versus the number of mismatches for pairs in this study with or without internal mismatches.

### *High mismatch destabilization energies predicted a low likelihood of unintended target reduction*

As observed for ASO_001 in Table 1, the most active unintended transcripts contained only a single terminal mismatch to the ASO. To test the hypothesis that hybridization free energy predicts the likelihood of reduction of an unintended target, hybridization free energies for each ASO:target pair were computed using the parameters of Turner and Mathews [42]. As shown above, these parameters were successful at predicting the destabilization free energies ($\Delta\Delta G°_{37}$) of mismatched versus matched ASO:target pairs. This nearest-neighbor model includes parameters for dangling ends, so each target site was extended 1 nt in each direction to allow for dangling end stabilization. Destabilization free energies ($\Delta\Delta G°_{37}$) were computed by subtracting the $\Delta G_{37}°$ of the intended target site from that of the unintended target site.

Most unintended targets were predicted to bind to the ASO with less affinity than the intended target. There were 21 exceptions, typically when a T in the ASO matched to A in the intended target and to G in the unintended target, and the dangling ends of the unintended target were more stabilizing than those of the intended target. The distribution of destabilization energy versus the number of mismatches for these 832 pairs is shown in Fig. 5. Although more mismatches resulted in greater destabilization, for any mismatch count, the range of $\Delta\Delta G°_{37}$ was very broad with internal mismatches resulting in greater destabilization than terminal mismatches.

Figure 6 plots the $IC_{50}$ ratio for each pair versus its predicted destabilization free energy ($\Delta\Delta G°_{37}$). If the unintended transcript was not reduced below 50% control at 10 times the $IC_{50}$ of the intended transcript, the ratio was reported as >10 and is plotted at a value of 10. Two trends are clear. First, most unintended transcripts were not reduced with an $IC_{50}$ within 10-fold that of the intended transcript. Second, transcripts that were reduced were associated with smaller destabilization free energies.

Figure 7 plots the fraction of unintended transcripts reduced with an $IC_{50}$ ratio <10 as a function of $\Delta\Delta G°_{37}$. For unintended transcripts with a stabilizing free energy, or a destabilizing free energy no more than 2 kcal/mol, 35/143 (24%) had an $IC_{50}$ within five-fold that of the intended transcript. In contrast, if the destabilization free energy was >4 kcal/mol only 4/407 (1.0%) of the unintended transcripts were reduced with an $IC_{50}$ less than five-fold that of the intended transcript.

Nearly 60% of the ASOs tested were fully phosphorothioate 3-10-3 gapmers with three constrained ethyl modifications on each end. The remaining ASOs were longer (17 or 20 nt) or contained 2′-O-methoxyethyl-modified wings, mixed 2′-O-MOE/cEt wings, altered gap sizes and positions (eg, 2-9-5 gapmer) and/or mixed phosphodiester/-phosphorothioate backbone. It was the $\Delta\Delta G°_{37}$ and not the oligonucleotide length or number of mismatches or modifications that affected likelihood of reduction of an unintended transcript, confirming the assertion that hybridization free energy is a primary driver of target selectivity.

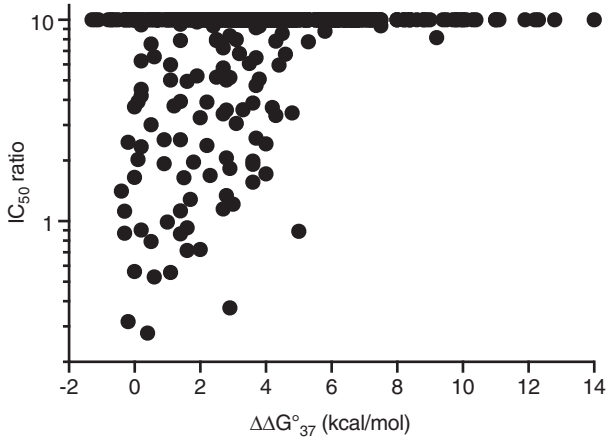


**FIG. 6.** Correlation of specificity of ASO reduction of unintended transcripts with predicted free energy for that ASO binding to the unintended target site. Ordinate is the $IC_{50}$ of the unintended transcript divided by the $IC_{50}$ of the intended transcript. Transcripts more than 10-fold less potent than the intended transcript are plotted at a value of 10. Around 735 (88%) of the unintended transcripts were more than 10-fold less potent than the intended transcript.

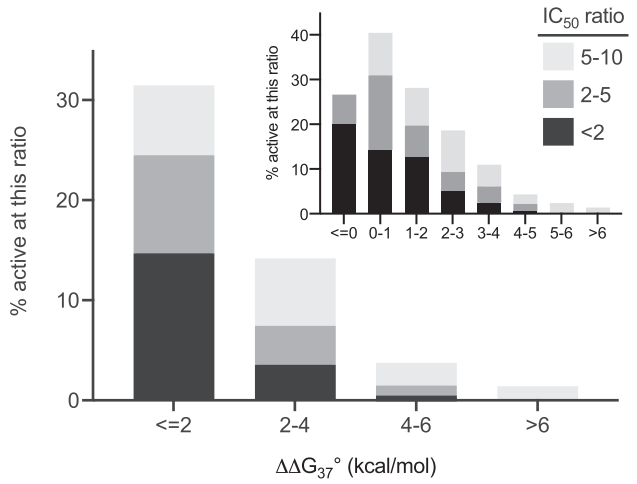


**FIG. 7.** Fraction of ASO:unintended transcript pairs with $IC_{50}$ within 10-fold that of the intended transcript as a function of predicted destabilization free energy. The first bin represents pairs predicted to be most stable with a binding constant within 25-fold of the perfect match and the last bin contains pairs predicted to be least stable with a binding constant more than $10^4$-fold less stable than the perfect match. A $\chi^2$ test of the data in Figure 7 substantiates the strong correlation of observed unintended transcript activity with predicted hybridization free energy at the unintended target site ($P < 10^{-15}$). *Inset*: Same data plotted with more free energy bins. The first bin ($\Delta\Delta G^{\circ}_{37} \leq 0$) contains pairs where the ASO is predicted to bind as strongly or more strongly to the unintended transcript than the intended transcript. In this case fully 20% of the unintended transcripts were reduced with a potency nearly as good as that of the intended transcript.

The correlation of mismatch destabilization with likelihood of reduction of an unintended transcript is similar to results reported by Lindow and colleagues [6,7]. Although they could not compare potency of intended and unintended targets, they report that unintended targets with observed reduction had significantly more favorable binding free energies than those that were not reduced. Similarly, Yoshida *et al.* [9] observed a strong correlation between likelihood of unintended target reduction and the complementarity measure for that unintended target.

These prior studies considered ASOs binding to unintended target sites with a single base bulge in the RNA. In the current study, most unintended target sites interrogated for 16-mers included only single internal mismatches or two terminal mismatches. For longer ASOs, an increased number of mismatches was investigated. Sites where the ASO would bind with a single base bulge were not tested.

This omission is not critical for the conclusions regarding the correlation of $\Delta\Delta G^{\circ}_{37}$ with the likelihood of reduction of an unintended transcript because only a range of $\Delta\Delta G^{\circ}_{37}$ values was necessary to test that hypothesis. Bulged loops of length one are predicted to destabilize more than single internal mismatches and much more than a single terminal mismatch [42]. Thus, inclusion of unintended target sites predicted to bind with a bulge in the ASO or the mRNA would have increased the number of more destabilizing pairs presented above. It is possible that a bulge could add additional RNA specificity beyond that resulting from free energy due to selectivity of RNase H1 for fully aligned duplex structures.

### *Mismatches in the gap were more likely to be selective*

To test if mismatch position affected the likelihood of reduction of an unintended transcript, $IC_{50}$ ratios were compared for pairs with and pairs without a mismatch in the DNA gap. Only 6/255 pairs (2.4%) with a mismatch in the gap had an $IC_{50}$ ratio <5 compared with 54/577 (9.3%) pairs without a mismatch in the gap and a ratio <5. Because internal mismatches are more destabilizing than terminal mismatches, the observation that fewer pairs with a mismatch in the gap were active compared with those with a mismatch in the wings may be due simply to the fact that wing mismatches may be terminal and thus less destabilizing than gap mismatches which are always internal.

Figure 8 compares the likelihood of reduction of unintended transcripts for only those pairs with nonterminal mismatches. Pairs with mismatches in the gap were less likely to be reduced than pairs with nonterminal mismatches in the wing. Supplementary Figure S6 makes the same comparison for all pairs as a function of destabilization free energy. When pairs with similar destabilization free energies were compared, mismatches in the gap were less likely to be reduced than no mismatch in the gap.

The observation that mismatches in the gap were less likely to result in reduction of an unintended transcript than nonterminal mismatches in the wings suggests that in addition to specificity provided by Watson–Crick hybridization, RNase H1 adds additional selectively against mismatches in the DNA gap presumably because many mismatches result in a structural defect near the cleavage site in the RNA:DNA duplex and this defect is disfavored by RNase H1 [51]. The role of RNAse H1 in mismatch selectivity was also reported by Rukov *et al.* who demonstrated reduction of gap size reduced activity against mismatched transcripts, but also affected RNHase H1 activity against the intended transcript resulting sometimes in

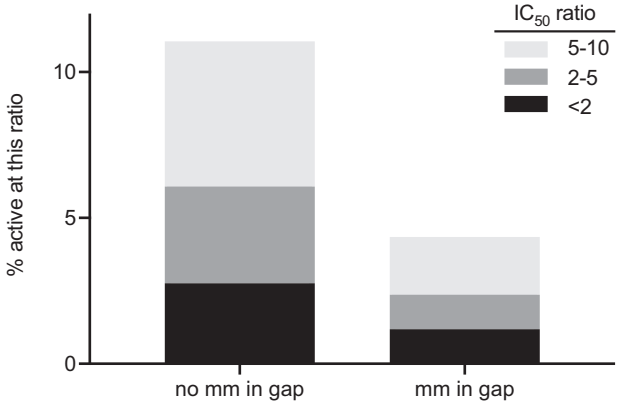


**FIG. 8.** Fraction of ASO:unintended transcript pairs with $IC_{50}$ within 10-fold that of the intended transcript for pairs with or without a mismatch in the gap. Only pairs with a nonterminal mismatch are included. 11% of the pairs with a mm in the wing and none in the gap were active ($IC_{50}$ within 10-fold that of the intended transcript), whereas 4% of those with a mm in the gap were active ($P < 0.05$, Fisher's exact test).

improved selectivity and sometimes in reduced selectivity but always in reduced activity toward the intended transcript [6].

Activity hit rates were assessed as a function of the mismatch position relative to the start of the gap (Supplementary Fig. S7). Although there were very few active pairs with a mismatch anywhere in the gap, it appears that mismatch position did not affect unintended transcript activity, except possibly that position 10 of the gap (3′ end of the gap) tolerated a mismatch better than a mismatch in other positions.

Pairs with a single terminal mismatch were evaluated to see if a mismatch on the 5′ end of the ASO affected activity more or less than on the 3′ end. Supplementary Figure S8 demonstrates that the position of a terminal mismatch did not substantially affect the likelihood of reduction of the unintended transcript.

### *Unintended transcript activity was independent of gene length and whether unintended site is intronic or exonic*

Activity hit rates were also compared for unintended transcripts where the ASO was expected to bind to an intronic or an exonic site. Only 3/53 pairs of an ASO with an exonic target site (6%) were reduced with an $IC_{50}$ within five-fold that of the intended target transcript. For intronic pairs, the rate was 57/779 (7.3%) (Supplementary Fig. S9). Kamola *et al.* [8] reported that intronic regions were markedly more susceptible to ASO silencing than exonic sequence. The current study contained only 53 unintended exonic sites and only three were active; thus the results in Supplementary Fig. S9 are statistically insignificant. However, current data support the hypothesis that unintended intronic sites are at least as likely as unintended exonic sites to result in unintended transcript reduction.

Finally, activity hit rates were evaluated as a function of length of the pre-mRNA (Supplementary Fig. S10) or the length of the mRNA (Supplementary Fig. S11). Little effect was observed.

### *Mismatch correction can, but does not always, increase activity at an unintended site*

Figure 4 demonstrates that many unintended transcripts were not reduced significantly at any concentration tested and most unintended transcripts, including several that were perfect matches to the ASO, were not reduced with an $IC_{50}$ within 10-fold that of the intended transcript. These results are consistent with the fact that not every ASO perfectly matched to an intended transcript reduces that transcript. This observation has been explained by differences in RNA accessibility due to secondary structure, protein binding, or processing kinetics [52–54]. Thus, a target site in an unintended transcript may be less accessible than that in the intended transcript or the unintended transcript itself may be less available for antisense targeting. Consequently, the unintended transcript may not be reduced by the ASO, even if the predicted duplex-binding free energy is strong.

To confirm that duplex stability is a strong predictor of the likelihood of reduction of the unintended transcript but target site availability also plays a role, a reciprocal experiment was performed. Two ASOs that were each active against at least one unintended transcript were selected. Dose/response data for these two ASOs showing response of intended and unintended transcripts are in Fig. 9. For each ASO, two unintended transcripts were reduced with $IC_{50}$ within 10-fold that of the intended transcript. In all cases, these active unintended transcripts were associated with small destabilization free energies (Table 2).

We hypothesized for the unintended transcripts that were reduced in Fig. 9, the ASO binding site was ‘‘accessible,’’ allowing for ASO binding and transcript reduction. To test this hypothesis, for each unintended transcript, the ASO sequence was corrected to be a perfect match to that unintended target site. $IC_{50}$ ratios for the ASO with the three active mismatched unintended transcript and the mismatch corrected ASO are listed in Table 3 with dose/response data in Supplementary Fig. S15.

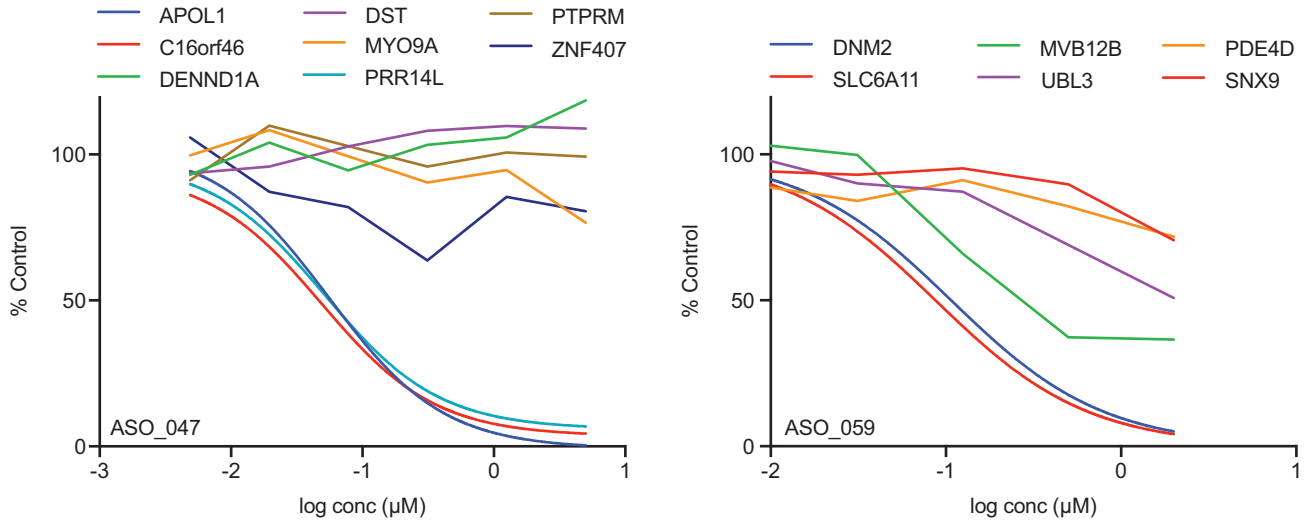


**FIG. 9.** Dose/response curves ASO_059 and ASO_047, two gen 2.5 16-mers showing reduction of both the intended transcript (*blue curves*) and several unintended transcripts. Reduction was measured 48 h after treatment in A431 cells by ‘‘free uptake.’’ These ASOs were selected because they have an unintended transcript whose reduction parallels that of the intended transcript. Only fitted curves are graphed. Supplementary Figures S12 and S13 show the same data with data points and error bars. $IC_{50}$ ratios and destabilization free energies for these pairs are shown in Table 2.

Table 2. Target Site Sequence, Destabilization Free Energy, and $IC_{50}$ Ratios for the ASO:Target Pairs in Figure 9

| *ASO:target* | *mm structure*[a] | *$IC_{50}$ ratio*[b] | *$\Delta\Delta G^{\circ}_{37}$ (kcal/mol)*[c] |
|---|---|---|---|
| ASO_047 | 5′ TGTTATATTTGATCCT 3′ | 1.0 | 0.0 |
| |   \|\|\|\|\|\|\|\|\|\|\|\|\|\|\|\| | | |
| *APOL1* | 5′CACAAUAUAAACUAGGAG | | |
| ASO_047 | 5′ TGTTATATTTGATCCT 3′ | 0.8 | 0.5 |
| |   \|\|\|\|\|\|\|\|\|\|\|\|\|\|\|\|**x** | | |
| *C16orf46* | 3′AACAAUAUAAACUAGGUG 5′ | | |
| ASO_047 | 5′ TGTTATATTTGATCCT 3′ | >10 | 3.6 |
| |   \|\|\|\|\|\|\|\|**x**\|\|\|\|\|\|\| | | |
| *DENND1A* | 3′ UACAAUAUACACUAGGAG5′ | | |
| ASO_047 | 5′ TGTTATATTTGATCCT 3′ | >10 | 3.8 |
| |   \|\|**x**\|\|\|\|\|\|\|\|\|\|\|\| | | |
| *DST* | 3′AACUAUAUAAACUAGGAU 5′ | | |
| ASO_047 | 5′ TGTTATATTTGATCCT 3′ | >10 | 1.9 |
| |   \|**x**\|\|\|\|\|\|\|\|\|\|\|\|\| | | |
| *MYO9A* | 3′UAUAAUAUAAACUAGGAA 5′ | | |
| ASO_047 | 5′ TGTTATATTTGATCCT 3′ | 1.0 | 1.0 |
| |   **x**\|\|\|\|\|\|\|\|\|\|\|\|\|\|\| | | |
| *PRR14L* | 3′AUCAAUAUAAACUAGGAA 5′ | | |
| ASO_047 | 5′ TGTTATATTTGATCCT 3′ | >10 | 6.3 |
| |   \|\|\|\|\|\|\|\|\|\|**x**\|\|\|\|\| | | |
| *PTPRM* | 3′GACAAUAUAAAAUAGGAU 5′ | | |
| ASO_047 | 5′ TGTTATATTTGATCCT 3′ | >10 | 4.2 |
| |   \|\|\|\|\|\|**x**\|\|\|\|\|\|\|\|\|\| | | |
| *ZNF407* | 3′GACAAUACAAACUAGGAU 5′ | | |
| ASO_059 | 5′ TAAGGGTTACTTTGCC 3′ | 1.0 | 0.0 |
| |   \|\|\|\|\|\|\|\|\|\|\|\|\|\|\|\| | | |
| *DNM2* | 3′CAUUCCCAAUGAAACGGU 5′ | | |
| ASO_059 | 5′ TAAGGGTTACTTTGCC 3′ | >10 | 5.9 |
| |   \|\|\|\|\|\|\|\|\|**x**\|\|\|\|\|\| | | |
| *SLC6A11* | 3′AAUUCCCAAUAAAACGGU 5′ | | |
| ASO_059 | 5′ TAAGGGTTACTTTGCC 3′ | 4.9 | 1.6 |
| |   \|**x**\|\|\|\|\|\|\|\|\|\|\|\|\|\| | | |
| *MVB12B* | 3′AAGUCCCAAUGAAACGGU 5′ | | |
| ASO_059 | 5′ TAAGGGTTACTTTGCC 3′ | >10 | 1.1 |
| |   **x**\|\|\|\|\|\|\|\|\|\|\|\|\|\|\| | | |
| *UBL3* | 3′CCUUCCCAAUGAAACGGA 5′ | | |
| ASO_059 | 5′ TAAGGGTTACTTTGCC 3′ | >10 | 5.0 |
| |   \|\|\|\|\|\|\|\|\|\|\|\|\|\|**x**\| | | |
| *PDE4D* | 3′CAUUCCCAAUGAAACCGU 5′ | | |
| ASO_059 | 5′ TAAGGGTTACTTTGCC 3′ | 1.1 | –0.3 |
| |   \|\|\|\|\|\|\|\|\|\|\|\|\|\|\|\| | | |
| *SNX9* | 3′AAUUCCCAAUGAAACGGU 5′ | | |

[a]Mismatched binding site on target RNA, including one additional nucleotide on each end. Upper strand is ASO and lower strand is RNA target site. Sites of mismatch are in *bold*.
[b]$IC_{50}$ (unintended transcript)/$IC_{50}$ (intended transcript).
[c]$\Delta G^{\circ}_{37}$ (unintended target site) − $\Delta G^{\circ}_{37}$ (intended target site).

For two of the three mismatched, unintended transcripts that were no more than 10-fold less potent than the parent (C16orf46 and MVB12B), correcting the mismatch to the unintended target site; improved potency two to seven-fold; for the third (PRR14L), correcting the mismatch resulted in negligible change in the dose/response curve. These improvements in potency with mismatch correction suggest the site was accessible and improving the hybridization energy improved potency.

For most of the unintended transcripts in Fig. 9 that had $IC_{50}$ ratios >10, correcting the mismatch did little to improve reduction of the unintended transcript suggesting that the ASO-binding site was inaccessible and the unintended target site was not susceptible to ASO activity whether the ASO was a perfect

TABLE 3. EFFECT OF MISMATCH CORRECTION ON REDUCTION OF UNINTENDED TARGETS FOR THE TWO ANTISENSE OLIGONUCLEOTIDES IN FIGURE 9

| *ASO:target* | *mm structure*[a] | *$IC_{50}$ ratio*[b] | *$\Delta\Delta G°_{37}$ (kcal/mol)*[c] | *Comment* |
|---|---|---|---|---|
| ASO_100 | 5′ AGTTATATTTGATCCT 3′ | 1.0 | 0.0 | Mismatch corrected |
| *PRR15L* | 3′ATCAATATAAACTAGGAA 5′ | | | |
| ASO_047 | 5′ TGTTATATTTGATCCT 3′ | 0.7 | 1.1 | Mismatched |
| *PRR14L* | 3′AUCAAUAUAAACUAGGAA 5′ | | | |
| ASO_101 | 5′ TGTTATATTTGATCCA 3′ | 1.0 | 0.0 | Mismatch corrected |
| *C16orf46* | 3′AACAATATAAACTAGGTG 5′ | | | |
| ASO_047 | 5′ TGTTATATTTGATCCT 3′ | 2.0 | 0.6 | Mismatched |
| *C16orf46* | 3′AACAAUAUAAACUAGGUG 5′ | | | |
| ASO_102 | 5′ TCAGGGTTACTTTGCC 3′ | 1.0 | 0.0 | Mismatch corrected |
| *MVB12B* | 3′ACCGTTTCATTGGGACTT 5′ | | | |
| ASO_059 | 5′ TAAGGGTTACTTTGCC 3′ | 7.4 | 4.2 | Mismatched |
| *MVB12B* | 3′AAGUCCCAAUGAAACGGU 5′ | | | |

[a]Mismatched binding site on target RNA, including one additional nucleotide on each end. Upper strand is ASO and lower strand is RNA target site. Sites of mismatch are in *bold*.
[b]Mismatched ASO/matched ASO.
[c]Mismatched pair—matched pair.

match or mismatched to this target site (data not shown). The exception was *ZNF407*, where the single mismatch with ASO_047 resulted in no activity but correcting the mismatch resulted in potency only two-fold weaker than the matched ASO with the intended target transcript (*APOL1*) (Supplementary Fig. S15 and Supplementary Table S8). Apparently, the ASO-binding site in *ZNF407* was accessible but the relatively high destabilization free energy reduced binding of ASO_047 to *ZNF407* or the C:A mismatch in position four of the gap prevented RNase H1 cleavage with ASO_047. Correcting this mismatch improved the hybridization free energy and resulted in reduction of this transcript.

### *Reducing hybrid stability by creating a mismatched ASO had the same effect as a mismatched target site*

The same three ASOs that corrected the mismatch to the unintended transcripts in Fig. 9 introduced a mismatch to the intended transcript and resulted in reduced or unchanged potency to that transcript (Supplementary Fig. S15 and Supplementary Table S9).

This observation that mismatch correction increased potency (Supplementary Figs. S14 and S15) and mismatch introduction decreased potency (Supplementary Fig. S16) is consistent with the hypothesis that more stable duplexes at the same site result in more potent compounds. To test this hypothesis, additional mismatched ASOs were designed that would reduce hybridization to the intended target site and modulate hybridization to the unintended target site. For each of the seven active target transcripts in Fig. 9, Supplementary Figs. S14 and S15, $IC_{50}$ ratios were calculated comparing the $IC_{50}$ of each mismatched ASO to that of the fully mismatch-corrected ASO. Predicted destabilization free energies were also calculated for each match/mismatch pair.

Figure 10 plots the $IC_{50}$ ratio (mismatched vs. matched ASO) versus the calculated $\Delta\Delta G°_{37}$ (mismatched—matched) for each pair and the inset plots the fraction of mismatched pairs reduced with an $IC_{50}$ ratio <10 as a function of $\Delta\Delta G°_{37}$. Figure 10 is very similar to Fig. 6; smaller destabilization free energies resulted in more potent reduction by the mismatched

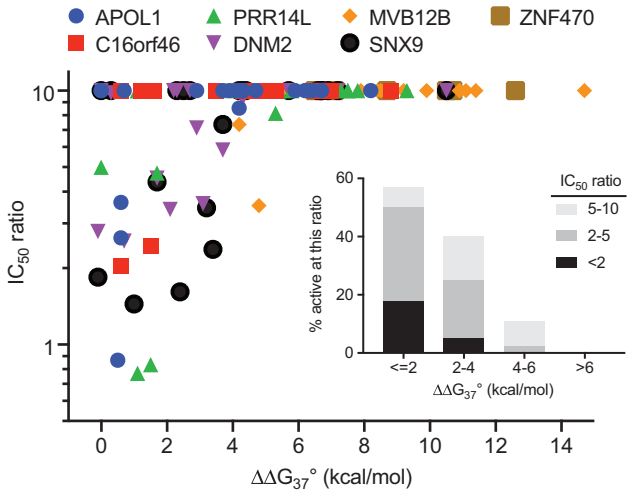


**FIG. 10.** Correlation of specificity of transcript reduction with matched and mismatched ASOs with predicted free energy destabilization for the mismatched ASO compared with the matched ASO. For each ASO, ordinate is the $IC_{50}$ of the mismatched ASO divided by $IC_{50}$ of the matched ASO. Mismatched ASOs more than10-fold less potent than the matched ASO are plotted at a value of 10. *Inset*: fraction of mismatched pairs reduced with an $IC_{50}$ ratio <10 as a function of $\Delta\Delta G°_{37}$.

ASO consistent with hybridization free energy being an important factor in determining whether or not an unintended transcript is reduced.

Although the data in Figs. 6 and 10 show a clear correlation of ASO selectivity with a small destabilization, a few outliers were observed. ASO_098_NRG2 and ASO_032_TFEB have destabilization energies of 2.9 and 5.0 kcal/mol, respectively, corresponding to changes in $K_D$ of 111- and 3,339-fold, respectively. Despite substantially reduced affinity of these ASOs for the mismatched RNA target sequence, these unintended transcripts were reduced with potency better than or equal to the intended transcript. This reduction, despite an unfavorable free energy destabilization suggests that in these rare cases factors other than hybridization play a role. Observation of nonhybridization-based mechanisms of ASO activity has been reported so these may be cases of nonhybridization-based transcript reduction [10,55–58], which seems to be rare for ASOs such as these that have passed standard tests of tolerability and activity.

Studies presented in Figs. 6 and 10 differ in that in Fig. 6, activity of a single ASO is compared for two target sites and in Fig. 10 two ASOs are compared for a single target site. Both approaches have been used previously to assess the effect of mismatches on antisense activity [6–8,27,59] and each of these experimental designs varies more than just the hybridization free energy. Varying ASO sequence can affect delivery of the ASO to the active site as well its nuclease resistance and ability to support RNase H1 cleavage of its perfect complement. On the other hand, varying the target site can affect target ''accessibility.'' Nonetheless, results in Fig. 10 are similar to those in Figs. 6 and 7 and support the conclusion that hybridization free energy is a primary determinant in the likelihood of reduction of a mismatched transcript.

### *Even nontoxic ASOs showed some nonspecificity and guidelines for identification of the most selective ASOs*

One proposed mechanism of hepatotoxicity for some high-affinity ASOs is reduction of a high number of unintended transcripts due to RNase H1-dependent RNA degradation [8,12,60]. The 96 ASOs in this study resulted from extensive screening of ASOs and showed no hepatotoxicity or immune stimulation in standard rodent toxicology studies. Despite the choice of potent, nontoxic ASOs for this study, reduction of a few unintended transcripts was observed, some with potency approaching that of the intended transcript demonstrating that even nontoxic ASOs can affect an unintended transcript. These data, however, suggest guidelines for ASO design to identify a selective ASO for a therapeutic or functional genomics application.

Given that likelihood of reduction of unintended transcripts is higher if binding to that transcript is predicted to be tighter, identification of the most likely ''off-targets'' can be reduced to calculation of expected free energy difference between binding to the intended and unintended target sites. Although, in general, mismatches destabilize duplexes and the more mismatches, the less stable the duplex, unintended target sites with a single mismatch can be destabilized as much as 7 kcal/mol (*ASO_004_CASK*) and, in contrast, two nonterminal mismatches can destabilize as little as 0.5 kcal/mol (*ASO_055_APOL2*) (Fig. 5 and Supplementary Table S5). Thus, counting potential mismatches is not an efficient way to predict the likelihood of reduction of an unintended transcript.

To assure the most problematic unintended transcripts are investigated, we propose that, for any ASO, unintended transcripts be interrogated for predicted $\Delta\Delta G^{\circ}_{37}$ compared with binding of the ASO to the intended transcript and those with the least destabilizing free energy be identified as the most likely unintended transcripts.

Data in Fig. 8 suggest for any destabilization free energy, a mismatch in the gap is less likely than a mismatch in the wing to result in reduction of an unintended transcript. Thus, unintended target sites with a mismatch in the gap are of less concern than those with a mismatch in the wing.

Once unintended transcripts with reasonable probability of reduction have been identified *in silico*, their expression and function should be assessed. If an unintended transcript is expressed only in a tissue where ASOs are inactive due to poor ASO distribution to that tissue, then that transcript may not be of concern. For example, if an ASO will be administered systemically, transcripts that are expressed only in the CNS may be of little concern because systemically administered ASOs do not cross the blood/brain barrier. Also, if a gene does not play an important role in a targetable tissue, it is of less concern. Knockout data of the gene may suggest that paralogs can replace that transcript.

Finally, selectivity is defined as the potency of the unintended transcript compared with the intended transcript. If an ASO has been optimized for reduction of its intended transcript, site accessibility and target-site availability have been optimized [61] and the ASO likely targets one of the most ''accessible'' sites for that transcript. The binding site on an unintended transcript has not been optimized so the likelihood of reduction of an unintended transcript will be smaller, even if the destabilization-free energy is small. The result will be a larger ratio of unintended to intended target transcript potencies, resulting in a more selective ASO. These guidelines are appropriate for ASOs of any length and modification.

### *Factors that affect ASO activity*

In addition to providing guidelines for identification of the most selective ASOs, these results provide insight into the factors affecting ASO activity at intended, as well as unintended transcripts. Clearly hybridization potential plays a key role. Hybridization potential includes thermodynamic stability of the ASO:target duplex and target-site accessibility, which is often attributed to RNAstructure, protein binding, and RNA processing kinetics. In addition to hybridization potential, the sequence or structure of the ASO:target pair affects the cleavage activity of RNase H1 [20] so sequence and structure of the DNA:RNA region of the ASO also plays a role, particularly when there are mismatches in the gap. We found little evidence that other factors such as transcript region played a substantial role. Intronic and exonic regions were equally targetable.

In summary, we demonstrated a strong correlation of mismatch destabilization with the likelihood of reduction of an unintended target transcript of an ASO. This result supports the use of mismatch-free energy prediction over mismatch number to select off targets most likely to be reduced.

Concentration dependence of reduction of these unintended transcripts should be measured in human cells and compared with that of the intended transcript to assess the likelihood reduction of that unintended transcript in humans.

### Author Disclosure Statement

The authors are employees of Ionis Pharmaceuticals, Inc.

### Funding Information

This work was funded by Ionis Pharmaceuticals, Inc.

### Supplementary Material

Supplementary Figure S1
Supplementary Figure S2
Supplementary Figure S3
Supplementary Figure S4
Supplementary Figure S5
Supplementary Figure S6
Supplementary Figure S7
Supplementary Figure S8
Supplementary Figure S9
Supplementary Figure S10
Supplementary Figure S11
Supplementary Figure S12
Supplementary Figure S13
Supplementary Figure S14
Supplementary Figure S15
Supplementary Figure S16
Supplementary Table S1
Supplementary Table S2
Supplementary Table S3
Supplementary Table S4
Supplementary Table S5
Supplementary Table S6
Supplementary Table S7
Supplementary Table S8
Supplementary Table S9

### References

1. Duell PB, RD Santos, BA Kirwan, JL Witztum, S Tsimikas and JJP Kastelein. (2016). Long-term mipomersen treatment is associated with a reduction in cardiovascular events in patients with familial hypercholesterolemia. J Clin Lipidol 10:1011–1021.
2. Wurster CD and AC Ludolph. (2018). Nusinersen for spinal muscular atrophy. Ther Adv Neurol Disord 11: 1756285618754459.
3. Benson MD, M Waddington-Cruz, JL Berk, M Polydefkis, PJ Dyck, AK Wang, V Plante-Bordeneuve, FA Barroso, G Merlini, *et al.* (2018). Inotersen treatment for patients with hereditary transthyretin amyloidosis. N Engl J Med 379: 22–31.
4. Suhr OB, T Coelho, J Buades, J Pouget, I Conceicao, J Berk, H Schmidt, M Waddington-Cruz, JM Campistol, *et al.* (2015). Efficacy and safety of patisiran for familial amyloidotic polyneuropathy: a phase II multi-dose study. Orphanet J Rare Dis 10:109.
5. Stojic L, ATL Lun, J Mangei, P Mascalchi, V Quarantotti, AR Barr, C Bakal, JC Marioni, F Gergely and DT Odom. (2018). Specificity of RNAi, LNA and CRISPRi as loss-of-function methods in transcriptional analysis. Nucleic Acids Res 46:5950–5966.
6. Rukov JL, PH Hagedorn, IB Hoy, Y Feng, M Lindow and J Vinther. (2015). Dissecting the target specificity of RNase H recruiting oligonucleotides using massively parallel reporter analysis of short RNA motifs. Nucleic Acids Res 43: 8476–8487.
7. Hagedorn PH, M Pontoppidan, TS Bisgaard, M Berrera, A Dieckmann, M Ebeling, MR Moller, H Hudlebusch, ML Jensen, *et al.* (2018). Identifying and avoiding off-target effects of RNase H-dependent antisense oligonucleotides in mice. Nucleic Acids Res 46:5366–5380.
8. Kamola PJ, JD Kitson, G Turner, K Maratou, S Eriksson, A Panjwani, LC Warnock, GA Douillard Guilloux, K Moores, *et al.* (2015). In silico and in vitro evaluation of exonic and intronic off-target effects form a critical element of therapeutic ASO gapmer optimization. Nucleic Acids Res 43: 8638–8650.
9. Yoshida T, Y Naito, H Yasuhara, K Sasaki, H Kawaji, J Kawai, M Naito, H Okuda, S Obika and T Inoue. (2019). Evaluation of off-target effects of gapmer antisense oligonucleotides using human cells. Genes Cells 24:827–835.
10. Gagnon KT and DR Corey. (2019). Guidelines for experiments using antisense oligonucleotides and double-stranded RNAs. Nucleic Acid Ther 29:116–122.
11. Yoshida T, Y Naito, K Sasaki, E Uchida, Y Sato, M Naito, T Kawanishi, S Obika and T Inoue. (2018). Estimated number of off-target candidate sites for antisense oligonucleotides in human mRNA sequences. Genes Cells 23: 448–455.
12. Burel SA, CE Hart, P Cauntay, J Hsiao, T Machemer, M Katz, A Watt, HH Bui, H Younis, *et al.* (2016). Hepatotoxicity of high affinity gapmer antisense oligonucleotides is mediated by RNase H1 dependent promiscuous reduction of very long pre-mRNA transcripts. Nucleic Acids Res 44: 2093–2109.
13. Ostergaard ME, AL Southwell, H Kordasiewicz, AT Watt, NH Skotte, CN Doty, K Vaid, EB Villanueva, EE Swayze, *et al.* (2013). Rational design of antisense oligonucleotides targeting single nucleotide polymorphisms for potent and allele selective suppression of mutant Huntingtin in the CNS. Nucleic Acids Res 41:9634–9650.
14. Dieckmann A, PH Hagedorn, Y Burki, C Brugmann, M Berrera, M Ebeling, T Singer and F Schuler. (2018). A sensitive in vitro approach to assess the hybridization-dependent toxic potential of high affinity gapmer oligonucleotides. Mol Ther Nucleic Acids 10:45–54.
15. Janas MM, MK Schlegel, CE Harbison, VO Yilmaz, Y Jiang, R Parmar, I Zlatev, A Castoreno, H Xu, *et al.* (2018). Selection of GalNAc-conjugated siRNAs with limited off-target-driven rat hepatotoxicity. Nat Commun 9:723.
16. Haeussler M, K Schonig, H Eckert, A Eschstruth, J Mianne, JB Renaud, S Schneider-Maunoury, A Shkumatava, L Teboul, *et al.* (2016). Evaluation of off-target and on-target scoring algorithms and integration into the guide RNA selection tool CRISPOR. Genome Biol 17:148.
17. Hagedorn PH, BR Hansen, T Koch and M Lindow. (2017). Managing the sequence-specificity of antisense oligonucleotides in drug discovery. Nucleic Acids Res 45:2262–2282.
18. Herschlag D. (1991). Implications of ribozyme kinetics for targeting the cleavage of specific RNA molecules in vivo: more isn't always better. Proc Natl Acad Sci U S A 88:6921–6925.

19. Jackson AL, SR Bartz, J Schelter, SV Kobayashi, J Burchard, M Mao, B Li, G Cavet and PS Linsley. (2003). Expression profiling reveals off-target gene regulation by RNAi. Nat Biotechnol 21:635–637.
20. Kielpinski LJ, PH Hagedorn, M Lindow and J Vinther. (2017). RNase H sequence preferences influence antisense oligonucleotide efficiency. Nucleic Acids Res 45:12932–12944.
21. Krueger U, T Bergauer, B Kaufmann, I Wolter, S Pilk, M Heider-Fabian, S Kirch, C Artz-Oppitz, M Isselhorst and J Konrad. (2007). Insights into effective RNAi gained from large-scale siRNA validation screening. Oligonucleotides 17:237–250.
22. Lima WF and ST Crooke. (1997). Binding affinity and specificity of Escherichia coli RNase H1: impact on the kinetics of catalysis of antisense oligonucleotide-RNA hybrids. Biochemistry 36:390–398.
23. Lindow M, HP Vornlocher, D Riley, DJ Kornbrust, J Burchard, LO Whiteley, J Kamens, JD Thompson, S Nochur, *et al.* (2012). Assessing unintended hybridization-induced biological effects of oligonucleotides. Nat Biotechnol 30:920–923.
24. Zagalak JA, M Menzi, F Schmich, H Jahns, AM Dogar, F Wullschleger, H Towbin and J Hall. (2015). Properties of short double-stranded RNAs carrying randomized base pairs: toward better controls for RNAi experiments. RNA 21:2132–2142.
25. Fontenete S, J Barros, P Madureira, C Figueiredo, J Wengel and NF Azevedo. (2015). Mismatch discrimination in fluorescent in situ hybridization using different types of nucleic acids. Appl Microbiol Biotechnol 99: 3961–3969.
26. Kaura M and PJ Hrdlicka. (2016). Efficient discrimination of single nucleotide polymorphisms (SNPs) using oligonucleotides modified with C5-pyrene-functionalized DNA and flanking locked nucleic acid (LNA) monomers. Chem Asian J 11:1366–1369.
27. Monia BP, H Sasmor, JF Johnston, SM Freier, EA Lesnik, M Muller, T Geiger, KH Altmann, H Moser and D Fabbro. (1996). Sequence-specific antitumor activity of a phosphorothioate oligodeoxyribonucleotide targeted to human C-raf kinase supports an antisense mechanism of action in vivo. Proc Natl Acad Sci U S A 93:15481–15484.
28. Altschul SF, W Gish, W Miller, EW Myers and DJ Lipman. (1990). Basic local alignment search tool. J Mol Biol 215: 403–410.
29. Langmead B, C Trapnell, M Pop and SL Salzberg. (2009). Ultrafast and memory-efficient alignment of short DNA sequences to the human genome. Genome Biol 10:R25.
30. Needleman SB and CD Wunsch. (1970). A general method applicable to the search for similarities in the amino acid sequence of two proteins. J Mol Biol 48:443–453.
31. Pearson WR and DJ Lipman. (1988). Improved tools for biological sequence comparison. Proc Natl Acad Sci U S A 85:2444–2448.
32. Smith TF, MS Waterman and WM Fitch. (1981). Comparative biosequence metrics. J Mol Evol 18:38–46.
33. Swayze EE, AM Siwkowski, EV Wancewicz, MT Migawa, TK Wyrzykiewicz, G Hung, BP Monia and CF Bennett. (2007). Antisense oligonucleotides containing locked nucleic acid improve potency but cause significant hepatotoxicity in animals. Nucleic Acids Res 35: 687–700.
34. Reuter JS and DH Mathews. (2010). RNAstructure: software for RNA secondary structure prediction and analysis. BMC Bioinformatics 11:129.
35. Kierzek E, A Ciesielska, K Pasternak, DH Mathews, DH Turner and R Kierzek. (2005). The influence of locked nucleic acid residues on the thermodynamic properties of 2'-O-methyl RNA/RNA heteroduplexes. Nucleic Acids Res 33:5082–5093.
36. Kierzek E, A Pasternak, K Pasternak, Z Gdaniec, I Yildirim, DH Turner and R Kierzek. (2009). Contributions of stacking, preorganization, and hydrogen bonding to the thermodynamic stability of duplexes between RNA and 2'-O-methyl RNA with locked nucleic acids. Biochemistry 48: 4377–4387.
37. Owczarzy R, Y You, CL Groth and AV Tataurov. (2011). Stability and mismatch discrimination of locked nucleic acid-DNA duplexes. Biochemistry 50:9352–9367.
38. Tolstrup N, PS Nielsen, JG Kolberg, AM Frankel, H Vissing and S Kauppinen. (2003). OligoDesign: optimal design of LNA (locked nucleic acid) oligonucleotide capture probes for gene expression profiling. Nucleic Acids Res 31: 3758–3762.
39. Hughesman CB, RF Turner and CA Haynes. (2011). Role of the heat capacity change in understanding and modeling melting thermodynamics of complementary duplexes containing standard and nucleobase-modified LNA. Biochemistry 50:5354–5368.
40. Mctigue PM, RJ Peterson and JD Kahn. (2004). Sequence-dependent thermodynamic parameters for locked nucleic acid (LNA)-DNA duplex formation. Biochemistry 43: 5388–5405.
41. Sugimoto N, N Satoh, K Yasuda and S Nakano. (2001). Stabilization factors affecting duplex formation of peptide nucleic acid with DNA. Biochemistry 40:8444–8451.
42. Turner DH and DH Mathews. (2010). NNDB: the nearest neighbor parameter database for predicting stability of nucleic acid secondary structure. Nucleic Acids Res 38: D280–D282.
43. Zhang DY, SX Chen and P Yin. (2012). Optimizing the specificity of nucleic acid hybridization. Nat Chem 4:208–214.
44. Manning GS. (2002). Electrostatic free energy of the DNA double helix in counterion condensation theory. Biophys Chem 101–102:461–473.
45. Schroeder SJ and DH Turner. (2009). Optical melting measurements of nucleic acid thermodynamics. Methods Enzymol 468:371–387.
46. Zuker M. (1994). Prediction of RNA secondary structure by energy minimization. Methods Mol Biol 25:267–294.
47. Tinoco I, Jr., PN Borer, B Dengler, MD Levin, OC Uhlenbeck, DM Crothers and J Bralla. (1973). Improved estimation of secondary structure in ribonucleic acids. Nat New Biol 246:40–41.
48. Ghosh S, S Takahashi, T Endoh, H Tateishi-Karimata, S Hazra and N Sugimoto. (2019). Validation of the nearest-neighbor model for Watson-Crick self-complementary DNA duplexes in molecular crowding condition. Nucleic Acids Res 47:3284–3294.
49. Martin P. (1995). Ein neuer Zugang zu 2′-O-Alkylribonucleosiden und eigenschaften deren oligonucleotide. Helv Chim Acta 78:486–504.
50. Seth PP, A Siwkowski, CR Allerson, G Vasquez, S Lee, TP Prakash, EV Wancewicz, D Witchell and EE Swayze. (2009). Short antisense oligonucleotides with novel 2′–4′

conformationaly restricted nucleoside analogues show improved potency without increased toxicity in animals. J Med Chem 52:10–13.
51. Lima WF, JB Rose, JG Nichols, H Wu, MT Migawa, TK Wyrzykiewicz, G Vasquez, EE Swayze and ST Crooke. (2007). The positional influence of the helical geometry of the heteroduplex substrate on human RNase H1 catalysis. Mol Pharmacol 71:73–82.
52. Mathews DH, ME Burkard, SM Freier, JR Wyatt and DH Turner. (1999). Predicting oligonucleotide affinity to nucleic acid targets. RNA 5:1458–1469.
53. Matveeva O, B Felden, A Tsodikov, J Johnston, BP Monia, JF Atkins, RF Gesteland and SM Freier. (1998). Prediction of antisense oligonucleotide efficacy by in vitro methods. Nat Biotechnol 16:1374–1375.
54. Pedersen L, PH Hagedorn, MW Lindholm and M Lindow. (2014). A kinetic model explains why shorter and less affine enzyme-recruiting oligonucleotides can be more potent. Mol Ther Nucleic Acids 3:e149.
55. Stein CA. (2001). The experimental use of antisense oligonucleotides: a guide for the perplexed. J Clin Invest 108: 641–644.
56. Crooke ST. (2000). Evaluating the mechanism of action of antiproliferative antisense drugs. Antisense Nucleic Acid Drug Dev 10:123–126; discussion 127.
57. Bennett CF and EE Swayze. (2010). RNA targeting therapeutics: molecular mechanisms of antisense oligonucleotides as a therapeutic platform. Annu Rev Pharmacol Toxicol 50: 259–293.
58. Liang XH, JG Nichols, CW Hsu, TA Vickers and ST Crooke. (2019). mRNA levels can be reduced by antisense oligonucleotides via no-go decay pathway. Nucleic Acids Res 47:6900–6916.
59. Woolf TM, DA Melton and CG Jennings. (1992). Specificity of antisense oligonucleotides in vivo. Proc Natl Acad Sci U S A 89:7305–7309.
60. Kamola PJ, K Maratou, PA Wilson, K Rush, T Mullaney, T Mckevitt, P Evans, J Ridings, P Chowdhury, *et al.* (2017). Strategies for in vivo screening and mitigation of hepatotoxicity associated with antisense drugs. Mol Ther Nucleic Acids 8:383–394.
61. Freier SM and AT Watt. (2007). Basic principles of antisense drug discovery. In: *Antisense Drug Discovery: Principles, Strategies and Applications*. Crooke ST, ed. CRC Press, New York, pp 117–141.

Address correspondence to:
*Susan M. Freier, PhD*
*Ionis Pharmaceuticals*
*2855 Gazelle Court*
*Carlsbad, CA 92010*
*USA*

*E-mail:* sfreier@ionisph.com

Received for publication January 13, 2020; accepted after revision January 30, 2020; published online March 3, 2020.